Color-Coded Phasor Analysis for Improved Retinal Disease Differentiation

A. Eskandarinasab[1*], F.J. Burgos-Fernández[1], L. Rey-Barroso[1], J. Pujol[1], M. Vilaseca[1]

[1]*Center for Sensors, Instruments and Systems Development, Universitat Politècnica de Catalunya, Rambla de Sant Nebridi 10, Terrassa, Barcelona*

https://www.cd6.upc.edu

Abstract: This study introduces two coloring methods for multispectral phasor analysis to enhance retinal health assessment. We captured spectral data from 102 retinas (50 diseased, 52 healthy) using a custom fundus camera and generated 2D phasor plots. Individual phasor coloring highlighted specific retinal structures, while dataset-wide coloring visualized overall health. Healthy retinas showed a red-blue pattern, and diseased retinas, a red-yellow-green palette. These coloring methods, combined with multispectral phasor analysis, offer the potential for enhanced retinal data visualization and diagnostic capabilities in ophthalmology.

1. Introduction

The retina is a crucial part of the human eye, serving as the light-sensitive layer at the back of the eye. Our entire vision relies on the proper functioning of the retina. If any damage occurs to this structure, it can result in significant vision loss or other serious visual impairments. Consequently, ophthalmologists conduct thorough examinations of the retina using specialized equipment, such as fundus cameras, to identify any potential symptoms of retinal disorders.

Traditional fundus cameras primarily capture images in RGB (red, green, blue) bands. These cameras offer satisfactory resolution and image quality, which are essential for ophthalmologists in diagnosing and monitoring eye conditions. However, with advancements in technology, new imaging devices based on multispectral cameras have been developed. Unlike standard fundus cameras, multispectral cameras can capture images across a range of different wavelengths, providing spectroscopic information rather than just color. This can reveal critical details that ophthalmologists can use for better diagnostic insights. In fact, multispectral imaging is not only beneficial in ophthalmology but is also widely utilized in various medical applications [1,2].

Despite the enhanced information provided by multispectral fundus cameras, interpreting the data can be challenging. This difficulty arises from the inter-band correlation, which makes it hard for the human eye to distinguish small differences in intensity across various spectral bands. To address this, phasor analysis is employed as a powerful tool to simplify the complexity of the spectral data. This technique converts the spectral information into a format that is more accessible and interpretable for human observers [3].

Phasor analysis enables the transformation of spectral data into two-dimensional plots, which allow for innovative ways to visualize multispectral images. For instance, we can color multispectral images to highlight different regions and structures of the retina, enhancing the visibility of critical features. Additionally, by analyzing phasor plots from multiple retinas, we can assign colors to each retina that reflect their health status, distinguishing between healthy and diseased conditions. This approach empowers ophthalmologists to focus on specific areas of interest and quickly assess the overall health of the retina by simply examining the colored images.

In this study, we investigate the advancements in retinal imaging through the use of multispectral cameras and phasor analysis. By transforming spectral data into more interpretable color representations, we demonstrate how these techniques can improve the assessment of retinal health, allowing for better differentiation between healthy and diseased conditions.

* *e-mail*: armin.eskandarinasab@upc.edu

2. Material and Methods

2.1. Multispectral Fundus Camera

Multispectral images were obtained using a custom-designed, multispectral fundus camera, as described in [4]. This device is equipped with an optical system that includes an array of LEDs, each emitting light at a specific peak wavelength in the visible and near-infrared range. It features two cameras: a high-resolution CMOS sensor (2048 x 2048 pixels, with a pixel size of 6.5 µm and a 16-bit depth) that captures 12 spectral images across a wavelength range of 416 to 955 nm, and a lower-resolution InGaAs camera (640 x 512 pixels, with a pixel size of 20 µm and a 14-bit depth) that captures images in three bands from 1025 to 1213 nm. Following post-processing and cropping for denoising and centering purposes, the final images retained dimensions of 1757 x 1757 pixels for the CMOS camera and 386 x 386 pixels for the InGaAs camera. In this study, the three near-infrared images from the InGaAs camera were excluded due to their lower resolution and higher noise levels compared to those captured by the CMOS sensor.

2.2. Data Collection

A dataset consisting of multispectral images from 102 retinas was utilized, including 50 cases of diseased retinas and 52 healthy cases, resulting in a total of 1,224 images. The diseased retinas exhibited various conditions, such as Age-related Macular Degeneration (AMD) (13), epiretinal membrane (6), retinal detachment (4), drusen deposits (5), and others (22). These images were collected at the Instituto de Microcirugía Ocular (IMO - Miranza Group) in Barcelona, Spain, and the Centre Universitari de la Visió (CUV) at the Universitat Politècnica de Catalunya in Terrassa, Spain [5].

2.3. Phasor Analysis

Phasor analysis was performed for each pixel within the spectral cube of a sample represented as (x, y, λ). Each spectrum is expressed as a complex number comprising real and imaginary components ($g_{x,y}$ + $is_{x,y}$) and is processed using a discrete Fourier transform [6]. The real and imaginary parts are defined as follows:

$$g_{x,y}(k)=\frac{\sum_{\lambda 0}^{\lambda n} I_{x,y}(\lambda) * \cos\left(\frac{2\pi k\lambda}{2}\right) * \Delta\lambda}{\sum_{\lambda 0}^{\lambda n} I_{x,y}(\lambda) * \Delta\lambda}, s_{x,y}(k)=\frac{\sum_{\lambda 0}^{\lambda n} I_{x,y}(\lambda) * \sin\left(\frac{2\pi k\lambda}{2}\right) * \Delta\lambda}{\sum_{\lambda 0}^{\lambda n} I_{x,y}(\lambda) * \Delta\lambda} \quad (1)$$

Here, λ_0 and λ_n denote the wavelengths of the first and last bands of the multispectral image, respectively (i.e. 416 to 955 nm). The variable n represents the number of spectral channels in the spectral cube, $\Delta\lambda$ indicates the bandwidth of a single channel, and k refers to the harmonic number. In this study, only harmonic 1 is examined, as finer details in the spectrum are more clearly observed in this harmonic compared to others.

2.4 Retina-Specific Phasor Coloring

Each spectrum in the multispectral image is represented as a point in a 2D phasor plot, where phasor analysis groups similar spectra together, linking each area of the plot to the corresponding spectral information. A specific color is assigned to each region of the phasor plot, allowing us to map these designated colors back to the original multispectral image, resulting in a visually appealing and interpretable representation. The color for each point is defined by adjusting its hue, saturation, and intensity. While various methods exist for coloring phasor plots [6], this study employs a radial coloring approach, treating the real (g) and imaginary (s) components as points in a polar coordinate system. In this method, the hue is determined by the angle, and the saturation is defined by the radius, with intensity set to a constant value of 1 throughout the image. This method is illustrated in in Fig. 1. Furthermore, the hue is normalized to a range of 0 to 1, ranging from magenta (corresponding to minimum angles), blue, cyan, green, yellow, …, to red at the maximum angles. Similarly, the saturation is also normalized between 0 and 1, with phasors having the maximum distance from the origin resulting in a saturation of 1, and those with the minimum distance having a saturation of 0.

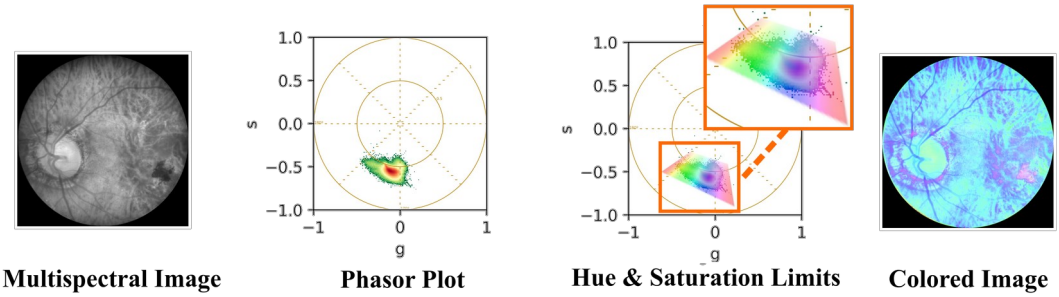

Figure 1: From left to right, the multispectral image contains detailed information about the retina across multiple wavelengths. This image is then transformed into a 2D phasor plot, in this case using harmonic 1, representing all pixels from a sample (retina). The limits for hue and saturation are established based on the values obtained from the phasor analysis. Each point in the phasor plot corresponds to a specific color, resulting in the final colored image.

2.5 Dataset-Wide Phasor Coloring

To establish a coloring system that reflects the health status of the retina, it is essential to consider all retinas in this dataset collectively. This involves calculating the average values for the real (g) and imaginary (s) components, referred to as (g_{avg}, s_{avg}). As illustrated in Fig. 2, the averaged values for healthy and diseased retinas are mostly separated from one another. Consequently, the limits for hue and saturation are determined based on the positions of these averaged values. Once the hue and saturation thresholds are established, they are applied to each image. The overall color of each image thus provides an indication of the retina's health status.

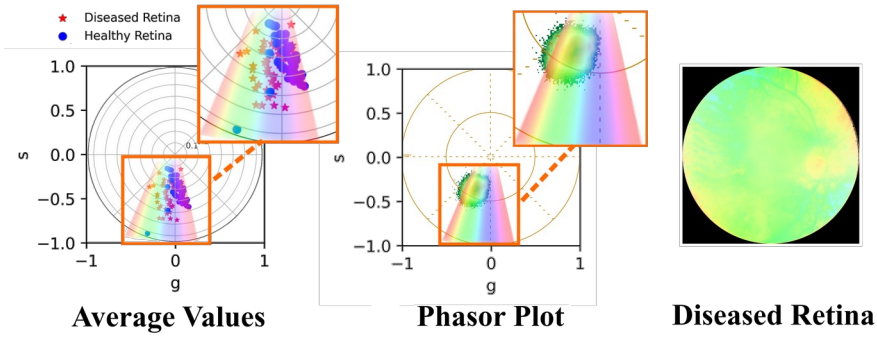

Figure 2: The hue and saturation limits are determined based on the averaged values from all samples (retinas). Once these limits are established, they are applied to the phasor plot, resulting in a colored image that highlights a diseased retina.

3. Results

By coloring each retina according to its phasor plot, different regions of the retina are enhanced, making structures such as the optic disc and veins more distinct and easily identifiable. This amplification facilitates a more straightforward analysis of these components. Fig. 3 presents several examples of this coloring technique.

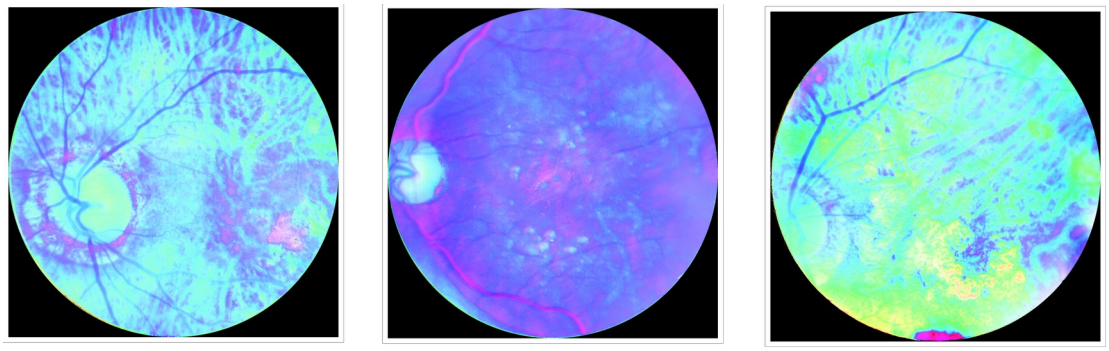

Figure 3: Examples of retina-specific phasor coloring to enhance visualization of specific retinal features, including the optic disc, retinal vessels, and etc. The first and third images display features indicative of AMD, while the middle image shows drusen deposits.

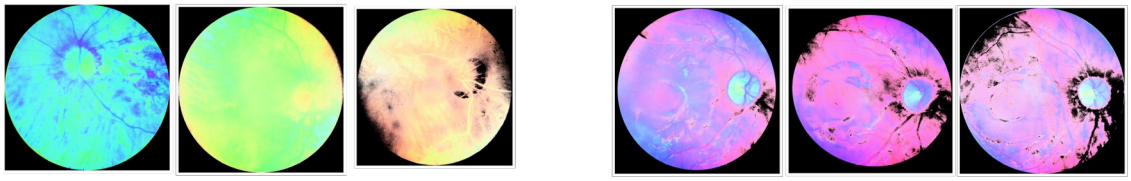

Figure 4: Comparison between diseased and healthy retinas after dataset-wide phasor coloring

When applying the coloring method based on dataset-wide phasor coloring, healthy retinas typically exhibit a red-blue color scheme, while diseased retinas display a red-yellow-green palette (Fig. 4). In instances where the phasor plots of healthy and diseased retinas are closely aligned, the resulting colors may also be similar, making it challenging to distinguish between the two based on overall coloring. It is important to note that some images may contain black pixels in the final colored output, indicating that the phasor plot for those images fell outside the established hue and saturation limits.

4. Conclusions

This study demonstrates the potential of multispectral imaging and phasor analysis in enhancing the assessment of retinal health by means of a color visualization approach. By utilizing a custom-designed multispectral fundus camera, we captured detailed spectral information from a diverse dataset of retinas, including both healthy and diseased cases. The application of phasor analysis allowed for the transformation of complex spectral data into interpretable color plots, facilitating the visualization of distinct retinal structures and enabling a more distinctive understanding of retinal health. The individual phasor coloring method amplified specific regions of the retina, making critical structures more identifiable, while the dataset-wide approach provided a broader context for assessing overall retinal health based on averaged spectral data, which could be alternatively used for screening purposes.

The findings indicate that while healthy retinas can be distinguished by a red-blue color scheme, challenges remain in differentiating between healthy and diseased retinas when their phasor plots are closely aligned. Additionally, the presence of black pixels in some images underscores the importance of establishing appropriate hue and saturation limits for accurate representation. Overall, this research highlights the value of integrating advanced imaging techniques and analytical methods as well as color-based approaches in ophthalmology. Future work may focus on refining these techniques and exploring their applicability in clinical settings to further enhance the understanding and treatment of retinal diseases.

Acknowledgments: Funded by European Union (HORIZON–MSCA–2022–DN, GA nº101119924–BE-LIGHT) and by MCIU /AEI/10.13039/501100011033 and FEDER, EU (Grant PID2023-147541OB-I00).

References

[1] W.M. MacCuaig, et al. "Development of multispectral optoacoustic tomography as a clinically translatable modality for cancer imaging." Radiology: Imaging Cancer, vol. 2(6), pp. e200066 (2020).

[2] X. Delpueyo, et al. "Multispectral imaging system based on light-emitting diodes for the detection of melanomas and basal cell carcinomas: a pilot study." Journal of biomedical optics, vol. 22(6), pp. 065006-065006 (2017).

[3] L. Malacrida, E. Gratton, D.M. Jameson. "Model-free methods to study membrane environmental probes: a comparison of the spectral phasor and generalized polarization approaches." Methods and applications in fluorescence, vol 3(4), pp. 047001 (2015).

[4] T. Alterini, et al. "Fast visible and extended near-infrared multispectral fundus camera." Journal of biomedical optics, vol 24(9), pp. 096007-096007 (2019).

[5] F.J. Burgos-Fernández, et al. "Reflectance evaluation of eye fundus structures with a visible and near-infrared multispectral camera." Biomedical optics express, vol. 13(6), pp. 3504-3519 (2022).

[6] W.Shi, et al. "Pre-processing visualization of hyperspectral fluorescent data with Spectrally Encoded Enhanced Representations." Nature Communications, vol. 11(1), pp. 726 (2020).